Triplet Excited State in Platinum−Acetylide Oligomers: Triplet Localization and Effects of Conformation

Ksenija Glusac, M. Erkan Köse,† Hui Jiang, and Kirk S. Schanze*

Department of Chemistry, University of Florida, Gainesville, Florida 32611-7200

Received: September 9, 2006; In Final Form: November 5, 2006

An experimental and theoretical investigation was carried out on a series of platinum−acetylide oligomers of the general structure Ph−C≡C−[PtL_2−C≡C−(1,4-Ph)−C≡C−]$_n$−PtL_2−C≡C−Ph (where n = 1, 2, 3, 4, 6; Ph = phenyl, 1,4-Ph = 1,4-phenylene; L = P(n−Bu)$_3$, and the geometry at Pt = trans). The objective of this work is to understand the geometry and electronic structure of the ground and triplet excited states of Pt−acetylide oligomers. The experiments carried out include temperature-dependent absorption and photoluminescence spectroscopy (80−298 K range) and ambient temperature transient absorption spectroscopy. Density functional theory (DFT) and time-dependent density functional theory (TD-DFT) calculations were carried out on several of the oligomers using the hybrid Becke's three-parameter functional with the B3LYP correlation functional and the SDD basis set. The combined experimental and theoretical results provide very clear evidence that the triplet excited state is localized on a chromophore consisting approximately of a single −[PtL_2−C≡C−(1,4-Ph)−C≡C−PtL_2]− repeat unit. DFT calculations indicate that in the ground state conformers that differ in the (rotational) orientation of the 1,4-phenylenes with respect to the plane defined by the $PtL_2(C)_2$ units (twisted = **t** and planar = **p**) are very close in energy (difference of <1 kcal·mol^{-1}). By contrast, in the triplet excited state, the **p** conformer is 3 kcal·mol^{-1} lower in energy than the **t** conformer. The torsional geometry change in the triplet state is reflected in the low-temperature phosphorescence spectra of the short oligomers, where separate emission bands are seen from the **t** and **p** conformers.

Introduction

Conjugated polymers and oligomers represent an important class of materials that show considerable promise for application in advanced electronic and optoelectronic devices.[1−6] Most research and development efforts on conjugated materials have focused on the properties and applications of organic polymers and oligomers.[5−8] However, the observation of very efficient electroluminescence from devices based on phosphorescent organometallic complexes has drawn attention to the importance of heavy-metal-enhanced singlet → triplet (S−T) intersystem crossing and phosphorescence in the development of advanced optoelectronic materials.[9,10] In addition to their application in electrophosphorescent devices,[11] organometallic complexes and polymers have also received attention as the active materials in photovoltaic devices[12,13] and as nonlinear absorbing chromophores.[14−17]

Platinum-containing complexes, oligomers, and polymers represent an important class of organometallic materials for optical and optoelectronic applications.[18,19] Platinum has a large spin−orbit coupling constant; consequently, π-conjugated materials that contain this element typically exhibit high triplet yields and efficient phosphorescence. Platinum−acetylide-based polymers and oligomers have received considerable attention because of their ease of synthesis combined with their favorable optical properties.[20−23] Whereas some of the research on Pt−acetylides is directed toward applications such as electrophorescence,[24] photovoltaics,[12,13] and nonlinear absorption,[14,15,20] these materials are particularly attractive for fundamental studies focused on the properties of the triplet state in π-conjugated electron systems. In particular, incorporation of the Pt−acetylide unit into an organic π-conjugated electron system leads to significant enhancement in the efficiency of S−T intersystem crossing combined with efficient phosphorescence. These properties allow one to apply spectroscopy easily to explore the triplet state and how it is influenced by factors such as conjugation length and energy.

Some of the most significant work in this area has been reported in collaborative efforts by Raithby, Khan, Friend, Köhler, and co-workers.[22−41] Their work confirmed that the excited states of Pt−acetylides are primarily localized on the organic chromophore system and that absorption and emission of light arise from π, π* transitions based on orbitals that are mainly localized on the organic chromophores (pπ) but contain contributions from Pt-based (dπ) orbitals. A comparison of the photophysics of Pt−acetylide polymers with their monomer analogs revealed that there is a higher level of electronic delocalization present in the polymers.[29] This observation provides clear evidence for delocalization through the Pt−acetylide unit, which is transmitted by dπ(Pt)−pπ(C) interactions.[29] This group also showed how the singlet−triplet splitting evolves with conjugation length and that the energy gap law holds for a diverse series of Pt−acetylide-based conjugated oligomers and polymers.[36,37]

We recently reported the synthesis and spectroscopic characterization of the series of monodisperse Pt−acetylide oligomers, Pt−***n***, illustrated in Chart 1.[42] These oligomers are of interest because they allow the investigation of the effects of conjugation length on the properties of the singlet and triplet

* Corresponding author. E-mail: kschanze@chem.ufl.edu. Phone: (352) 392-9133. Fax: (352) 392-2395. Web site: http://www.chem.ufl.edu/~kschanze.

† Present address: National Renewable Energy Laboratory, 1617 Cole Boulevard, Golden, Colorado 80401.

10.1021/jp065892p CCC: $37.00
Published on Web 01/18/2007

CHART 1

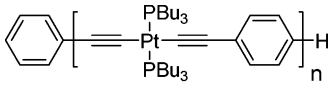

Pt-n n = 2-5, 7

excited states. In our earlier communication, we reported the effects of conjugation length on the absorption, fluorescence, and phosphorescence spectra of the series.[42] On the basis of the effects of conjugation length on the energies of the various spectroscopic transitions, we concluded that there is a substantial degree of delocalization in the singlet excited state whereas the triplet exciton is confined to a chromophore that encompasses only a small portion of a moderately long oligomer chain. In the present article, we describe the results of a more complete spectroscopic and theoretical analysis of the Pt−***n*** series of oligomers. In particular, temperature-dependent absorption and phosphorescence spectroscopy was carried out, and the results provide clear evidence that the conformation of phenylene repeat units in the Pt−acetylide chains has a strong influence on the absorption and phosphorescence energies. Density functional theory (DFT) calculations aid the interpretation of the spectroscopic data, and the results strongly suggest that at low temperatures the all-planar conformation of the oligomers predominates whereas at higher temperature a geometry in which the square-planar Pt−acetylide units and the phenylene units are oriented perpendicularly is populated. Transient absorption spectroscopy is used to generate the absolute triplet−triplet absorption spectra, $\epsilon_T(\lambda)$, and the results support the notion of a triplet exciton that is confined to a chromophore consisting of a single −[PtL_2−C≡C−Ph−C≡C−PtL_2]− repeat unit. The DFT calculations support this model, suggesting that localization is partially driven by a quinoidal geometric distortion that is localized in the excited 1,4-diethynylphenylene unit.

Experimental

Materials. The synthesis and characterization of the series of Pt−acetylide oligomers were reported previously.[42] Low-temperature spectroscopy was carried out with samples dissolved in 2-methyltetrahydrofuran (2-MTHF) that was purified by distillation from CaH_2.

Variable-Temperature Spectroscopic Measurements. Ultraviolet−visible absorption spectra were obtained using a Varian Cary 100 spectrophotometer. Corrected steady-state emission spectra were recorded on a SPEX F112 fluorescence spectrometer. The variable-temperature emission measurements were carried out by cooling samples in an Oxford Instruments DN-1704 optical cryostat. The optical density of the samples for emission measurements was adjusted to approximately 0.2 at the excitation wavelength. The samples were degassed by four repeated freeze−pump−thaw cycles on a high-vacuum line.

Transient Absorption Spectroscopy. Transient absorption spectroscopy was carried out on an instrument that has been described previously.[43] Samples were contained in a cell that holds a total volume of 10 mL, and the contents were continuously recirculated through the pump−probe region of the cell. Samples were degassed by argon purging for 30 min. Excitation was provided by the third harmonic output of a Nd:YAG laser (355 nm, Spectra Physics, GCR-14). Typical pulse energies were 5 mJ·pulse^{-1}, which corresponds to an irradiance in the pump−probe region of 20 mJ·cm^{-2}. Triplet−triplet molar extinction coefficients ($\Delta\epsilon$) were determined by an energy-transfer method from the Pt−acetylide oligomers to pyrene.[44] The Pt−acetylide solutions had an absorption of 0.6 at the excitation wavelength (355 nm), and the concentration of pyrene was 3×10^{-4} M. The efficiency for the energy-transfer process (η_{EnT}) was calculated using eq 1:

$$\eta_{EnT} = \frac{k_{EnT}[Pyr]}{k_{EnT}[Pyr] + k_d} \quad (1)$$

Here, k_d represents the rate of decay of the triplet excited state of Pt−acetylide in the absence of pyrene, and it was calculated from the excited-state decay kinetics observed at 660 nm. The decay obtained when pyrene is added to the oligomer solution gave $k_{EnT}[Pyr] + k_d$ as a pseudo-first-order rate constant. The triplet−triplet molar extinction coefficient was obtained from eq 2:

$$\Delta\epsilon_{Pt} = \frac{\eta_{EnT}\Delta\epsilon_{Pyr}\Delta A_{Pt}}{\Delta A_{Pyr}} \quad (2)$$

In this equation, ΔA_{Pt} is ΔA at 660 nm extrapolated to time zero, whereas ΔA_{Pyr} is ΔA at 415 nm at a delay time when the Pt−***n*** triplet has fully decayed but the pyrene triplet has not substantially decayed (ca. 5 μs). The molar extinction coefficient of the triplet−triplet absorption of pyrene was taken from the literature ($\Delta\epsilon_{Pyr}$ = 36 400 M^{-1}·cm^{-1} at λ = 415 nm).[44]

Computational Methods. All calculations were carried out using DFT as implemented in Gaussian 03.[45] Geometries were optimized using the hybrid Becke's three-parameter functional with the Lee, Yang, and Parr correlation functional (B3LYP)[46−48] along with the SDD basis set, which employs the Stuttgart−Dresden relativistic effective core potential with explicit treatment of platinum and the Dunning−Huzinaga valence double-ζ basis set for the other atoms. Initially the 6-31G+(d,p) basis set was used for C, H, and P. However, an analysis of the electronic structure results of the oligomers revealed no significant differences between the results of the two approaches; therefore, the SDD basis set was used throughout all of the calculations, saving considerable computational time. For Pt−**2**, calculations were carried out for both relaxed and symmetry-restricted forms. The **t** conformers were optimized with C_{2h} symmetry, whereas all other conformers were optimized under D_{2h} or C_s symmetry constraints. The optimized structures for the conformational isomers of Pt−**2** were characterized by vibrational frequency calculations. Energy minima for each stationary point were characterized either by the absence of imaginary frequencies or by the very low imaginary frequencies corresponding to phenyl rotation. Time-dependent DFT calculations were performed for all of the optimized structures at the same level of theory with the same basis set. Simulation of the phosphorescence spectrum of Pt−**2** was carried out according to the method described by Gierschner and co-workers.[49]

Results

Structure and Conformational Considerations. The platinum oligomers that are the focus of this investigation are illustrated in Chart 1. The oligomers each contain a repeating unit consisting of a square-planar *trans*-Pt$(PBu_3)_2(C)_2$ unit alternating with 1,4-diethynylphenylene. An important component of this work concerns the conformation of the conjugated backbone. To facilitate a discussion of this issue, we will define two limiting conformations with respect to the rotation of the phenylene groups around the long axis of the molecule.[50] By reference to Scheme 1, we define "twisted" (**t**) as the conforma-

SCHEME 1

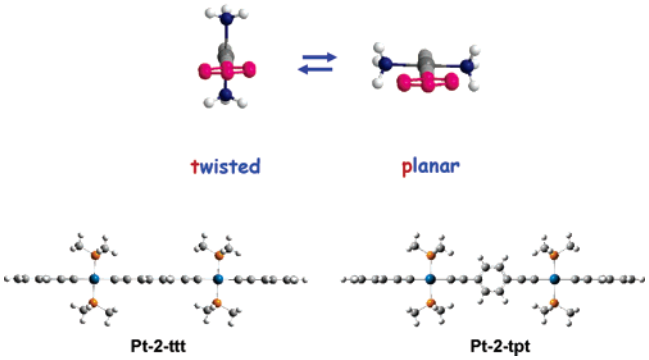

tion in which the planes defined by the square-planar *trans*-Pt-$(PBu_3)_2(C)_2$ and phenylene units are perpendicular and "planar" (**p**) as the conformation in which these two units are coplanar. Scheme 1 also illustrates examples of this nomenclature as applied to two important conformers of oligomeric Pt−**2**. Specifically, Pt−**2**−**ttt** is the conformer of Pt−**2** in which the three phenyl rings are twisted 90° relative to the planes defined by the two *trans*-$Pt(PBu_3)_2(C)_2$ units. In Pt−**2**−**tpt**, the central phenylene ring is oriented coplanar relative to the planes defined by the two *trans*-$Pt(PBu_3)_2(C)_2$ units, whereas the two terminal phenylene units are twisted 90°.

Variable-Temperature Absorption Spectroscopy. Figure 1 shows the absorption spectra for the series Pt−**2**−Pt−**5** obtained in 2-MTHF solution over a temperature range of 90−298 K. The absorption spectrum of each oligomer is dominated by a strong band with a maximum in the near-UV region arising from the long-axis-polarized π, π^* transition. The absorption maximum red shifts with increasing oligomer length, consistent with a degree of π delocalization in the ground and first singlet excited states. Interestingly, for all of the oligomers, the dominant absorption band red shifts, narrows in bandwidth, and becomes more intense (increase in ϵ_{max}) with decreasing temperature. This behavior is similar to that seen in many π-conjugated organic oligomers and polymers, where it has been ascribed to changes in conformation of the repeating units in the π-conjugated system.[51−53] We believe that a similar effect is operating in the Pt−acetylide oligomers; that is, as the temperature is decreased, a single conformational state of the oligomers predominates, giving rise to increased π conjugation and a lowering of the HOMO−LUMO gap. The different conformational states are believed to arise as a result of rotation of the phenylene rings relative to the planes defined by the square-planar PtP_2C_2 units. The origin of these effects is explored more fully below, where the results of quantum chemical calculations are presented.

Variable-Temperature Photoluminescence Spectroscopy. Further insight into the effect of temperature on the spectroscopy of the Pt−acetylide oligomers is provided from emission studies carried out over temperatures ranging from 80−298 K. As reported previously, each of the Pt−***n*** oligomers (n = 2−5,7) exhibits a moderately intense phosphorescence band with $\lambda_{max} \approx 520$ nm (λ_{max} corresponds to the 0−0 band).[42] The position of the 0−0 phosphorescence band is nearly independent of oligomer length, consistent with the triplet exciton being spatially confined to a segment of the oligomer. The emission envelope also features a manifold of vibronic sub-bands at lower energy from the 0−0 band. The origin of the vibronic progression is revealed by a Franck−Condon band analysis, which is described in a later section. This analysis shows that the spectral progression arises from the coupling of the excitation with at least seven fundamental vibrational modes with frequencies ranging from 93 to 2165 cm^{-1}. The weaker vibronic bands that appear at lower energy correspond to combinations of these fundamental modes.

The temperature dependence of the phosphorescence of the Pt−***n*** oligomers was studied over the temperature range from 90 to 298 K in 2-MTHF, which forms an amorphous glass at ca. 120 K. The phosphorescence of the oligomers changes relatively little for temperatures above the solvent glass point (130−298 K), and thus the spectra for this range are not shown. However, as shown in Figure 2, upon cooling the samples through and below the solvent glass point (130−90 K) interesting changes are seen in the emission spectra. Focusing first on Pt−**2** at 120 K, the emission envelope appears as a single 0−0 band (λ = 519 nm) with a broad vibronic progression at longer wavelengths. However, at lower temperature the 0−0 band broadens, and a shoulder is resolved at shorter wavelength. At 90 K, the intensity of the high-energy shoulder is ca. 60% compared to that of the main 0−0 band. The shoulder is shifted ca. 660 cm^{-1} (1.8 kcal·mol^{-1}) to higher energy compared to the main 0−0 band. It is quite evident from this series of temperature-dependent spectra that in the solvent glass Pt−**2** exhibits luminescence from several states and as outlined below these states are believed to be conformers that cannot interconvert during the lifetime of the triplet state in the frozen glass.

Similar effects are observed in the phosphorescence spectra of Pt−**3** over the 130−90 K range. However, interestingly for Pt−**3** the high-energy shoulder that appears below 120 K in the solvent glass has an intensity that is only 25% relative to that of the main 0−0 band. An inspection of the variable-temperature emission spectra for the longer oligomers (Pt−**4** and Pt−**7**) shows that for these systems the high-energy emission component is hardly visible at low temperature in the 2-MTHF glass. For both of the longer oligomers in the low-temperature solvent glass, there is only a slight broadening observed on the high-energy side of the 0−0 band. The trend observed across the series suggests that for the longer oligomers there is a mechanism operating that allows the excitation to migrate away from high-energy conformations, giving rise to the homogeneous emission band shape characteristic of the low-energy conformation. As outlined in more detail below, we believe that this process is intrachain triplet exciton transfer.

Emission excitation studies provide clear evidence that the splitting of the 0−0 emission band that occurs in the emission spectra of the Pt−***n*** oligomers below 120 K arises as a result of the existence of noninterconverting conformers in the frozen solvent glass. Figure 3 shows the emission excitation spectra of Pt−**2** obtained while monitoring the emission at 497 nm (the peak of the high-energy shoulder) and 517 nm (λ_{max} for the main 0−0 band). Two nearly identical, well-resolved excitation profiles are obtained, each featuring a distinct 0−0 band with a vibronic progression at higher energy. Interestingly, the excitation band that is obtained with λ_{em} = 497 nm (the high-energy shoulder) is shifted ca. 1490 cm^{-1} (4.2 kcal·mol^{-1}) to higher energy compared to the excitation band obtained with λ_{em} = 517 nm. The emission spectra that are also shown in Figure 3 show that it is possible to selectively excite the different Pt−**2** conformers present in the low-temperature glass to produce distinct emission spectra (i.e., photoselection).

In particular, with λ_{ex} = 340 nm, an emission profile with a 0−0 band at ca. 500 nm is observed, whereas with λ_{ex} = 385 nm, a similar emission profile is seen, but the 0−0 band is shifted to 519 nm. Note also that the spectrum obtained with the longer excitation wavelength is considerably better resolved

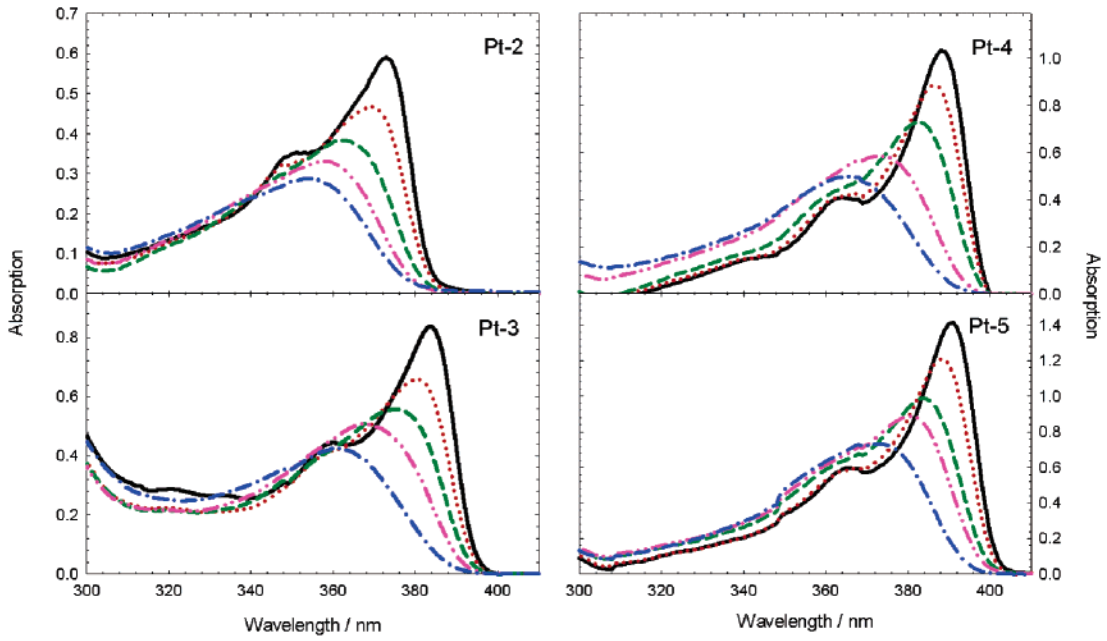

Figure 1. Variable-temperature absorption spectra of Pt−acetylide oligomers Pt−**2** through Pt−**5**: (−) $T = 90$ K, (···) 120 K, (− − −) 190 K, (− ·· −) 250 K, (− · −) 298 K.

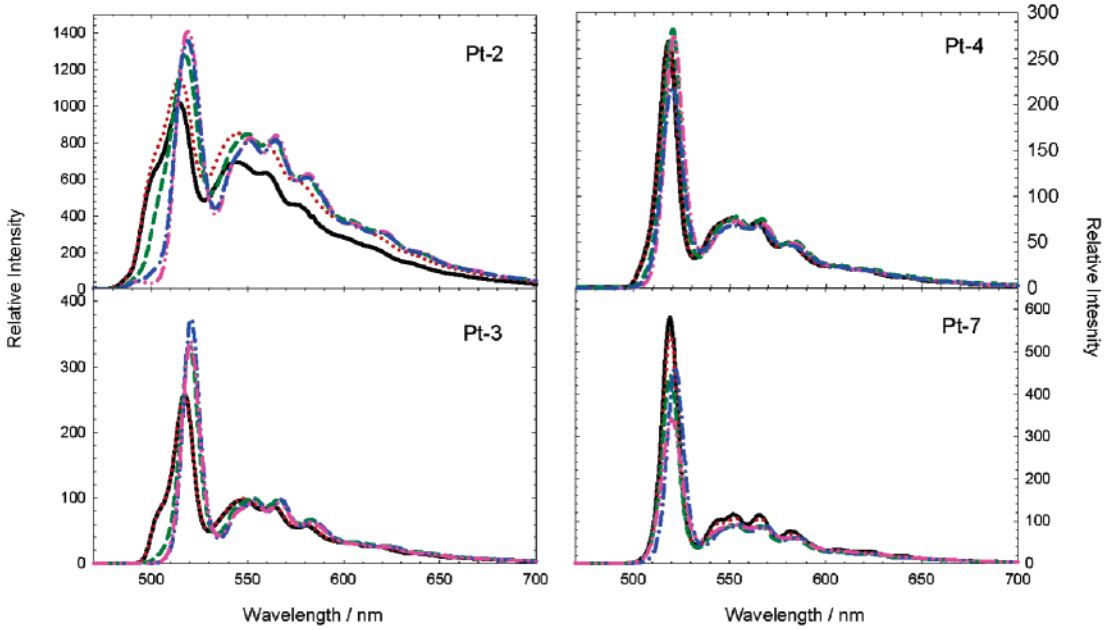

Figure 2. Variable-temperature phosphorescence spectra for oligomers Pt−**2** through Pt−**4** and Pt−**7**: (−) $T = 90$ K, (···) 100 K, (− − −) 110 K, (− ·· −) 120 K, (− · −) 130 K.

(narrower vibronic band widths), suggesting that low-energy excitation selectively excites a homogeneous population of conformers. Principal component analysis of Pt−**2** (80 K) emission spectra obtained at a variety of excitation wavelengths suggests that the excitation wavelength-dependent emission spectra can be reconstructed by using just two principal emission components with spectra similar to those shown in Figure 3.[54,55] This observation suggests that the wavelength-dependent excitation and emission profiles are determined by the existence of two distinct conformers that are frozen in the glass. Very similar observations were made in wavelength-dependent excitation and emission spectra of the longer oligomers (Pt−**3** and Pt−**4**, data not shown).[56]

It is evident from the temperature-dependent absorption and emission studies outlined above that in solution the Pt−***n*** oligomers exist in different conformational states and that the population distribution of the conformers is influenced strongly by temperature. A second point that is crucial to fully explaining the observations made in the photoluminescence spectroscopy is the notion that the triplet state is spatially confined in the oligomers. In the next section, we present the results of ambient-temperature transient absorption studies that provide clear evidence that the triplet state in these Pt−acetylides is spatially confined.

Transient Absorption Spectroscopy: Evidence for Triplet-State Localization. Transient absorption spectroscopy was carried out on the series of Pt−***n*** oligomers with the objective being to quantify the triplet−triplet absorption spectra and to provide further information on the structure of the triplet exciton. For each oligomer, excitation at 355 nm produces a strong

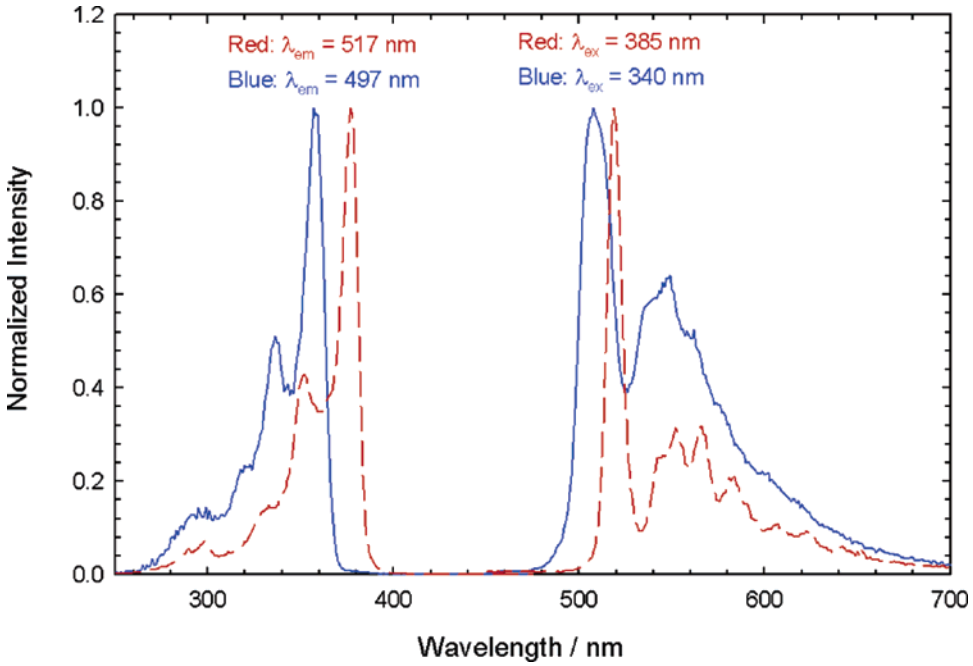

Figure 3. Emission and emission excitation spectra for Pt−acetylide oligomer Pt−**2**. Excitation spectra recorded with λ_{em} at 497 nm (−) and 517 nm (− − −). Emission spectra recorded with λ_{ex} at 340 nm (−) and 385 nm (− − −).

transient absorption signal due to the triplet state that decays with a lifetime of ca. 10 μs. The set of difference absorption spectra shown in Figure 4a for Pt−**3** is representative of the entire series of oligomers. In particular, the difference spectrum is characterized by a negative difference absorption band in near-UV combined with a broad absorption band with a maximum between 600 and 700 nm. The negative difference absorption in the near-UV corresponds to bleaching of the ground-state absorption band that is assigned to the π, π^* (S_0-S_1) transition. The broad visible absorption band is due to T_1-T_n absorption by the triplet excited state. The difference spectrum shown for Pt−**3** in Figure 4a is very similar to that of the polymer with the same repeat unit structure, $[-PtL_2-C\equiv C-Ph-]_n$ (L = PBu_3, Ph = 1,4-phenylene),[57] which shows that the difference spectrum is characteristic of the triplet exciton state in the Pt−acetylide oligomers and polymers.

To generate absolute absorption spectra for the triplet excited state oligomers, the energy-transfer method was used to determine the concentration of the triplet excited state produced by laser excitation.[44] Given this information, it is possible to determine the difference molar absorptivity spectrum $\Delta\epsilon(\lambda) = \epsilon_T(\lambda) - \epsilon_{gs}(\lambda)$, where $\epsilon_T(\lambda)$ is the absorption spectrum of the triplet excited state oligomer and $\epsilon_{gs}(\lambda)$ is the absorption spectrum of the ground state. Finally, addition of the ground-state absorption spectrum to the difference molar absorptivity spectrum allows one to recover the absolute absorption of the triplet excited state, that is, $\epsilon_T(\lambda) = \Delta\epsilon(\lambda) + \epsilon_{gs}(\lambda)$.

The acceptor for the energy-transfer studies was pyrene, which was chosen because it does not absorb appreciably at 355 nm, its triplet energy is below that of the oligomers (E_T(pyrene) ≈ 48 kcal·mol^{-1} vs E_T(Pt−***n***) ≈ 55 kcal·mol^{-1}), and it has a strong triplet−triplet absorption at λ = 415 nm ($\Delta\epsilon$ = 36 400 M^{-1}·cm^{-1}).[44] Figure S-1 in Supporting Information illustrates transient absorption data for a solution that contains Pt−**3** and pyrene, and the method used to determine $\Delta\epsilon(\lambda)$ from the data is described in the Experimental Section.

Figure 4b shows the absolute absorption spectra of the triplet excited state ($\epsilon_T(\lambda)$) for the series of Pt−***n*** oligomers recovered as described above. Each spectrum features the broad band in the 600−700 nm region that is due to the T_1-T_n absorption; there is some variance across the series (which likely arises in part because of experimental uncertainty in $\Delta\epsilon$ estimated at ±15%), but the absorptivity generally falls in the range of (60−

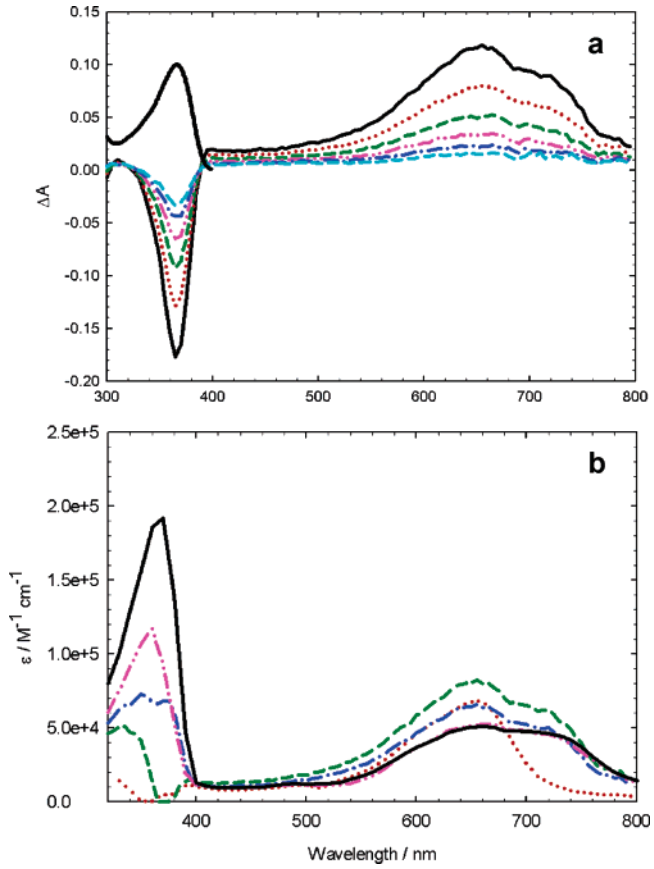

Figure 4. (a) Transient absorption spectrum of Pt−**3**: (−) t = 0 μs, (···) 3.2 μs, (− − −) 6.4 μs, (− ·· −) 9.6 μs, (− · −) 12.8 μs, (− − −) 16.0 μs. Solid black line: ground-state absorption spectrum of Pt−**3**. (b) Absolute triplet-state absorption spectra for Pt−***n*** oligomers computed as described in the text: (···) Pt−**2**, (− − −) Pt−**3**, (− · −) Pt−**4**, (− ·· −) Pt−**5**, (−−) Pt−**7**.

SCHEME 2

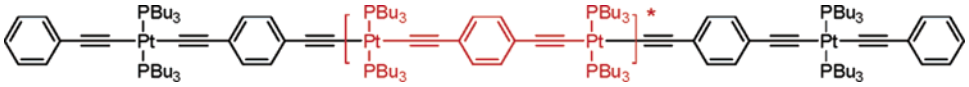

80) × 10^3 M^{-1}·cm^{-1}. These values are comparable to those observed in a recent study of Pt−acetylide complexes of the type aryl−C≡C−Pt(PBu_3)$_2$−C≡C−aryl.[58] In addition to the T_1−T_n band, an absorption feature that becomes more intense with oligomer length is observed with $\lambda_{max} \approx 380$ nm, which closely corresponds to the S_0−S_1 absorption of the ground-state oligomer. Careful inspection of the data shows that this transition is nearly absent in Pt−**2** and very weak in Pt−**3** but that its intensity rapidly increases for Pt−**4**, Pt−**5**, and Pt−**7**. We believe that this transition arises in the longer excited-state oligomers because the triplet state is confined to a short segment and the remainder of the oligomer acts as a ground-state chromophore that exhibits its characteristic S_0−S_1 transition at $\lambda \approx 380$ nm. Using the value of the ground-state molar absorptivity per repeat unit (∼40 × 10^3 M^{-1}·cm^{-1}),[42] the intensity of the residual absorption in the S_0−S_1 region for the excited-state oligomers can be used to estimate the spatial extent of the triplet exciton. This estimate leads us to the hypothesis that the triplet exciton encompasses a chromophore that consists approximately of −[PtL_2−C≡C−Ph−C≡C−PtL_2]−. For example, in Pt−**4** we envision the triplet exciton to be confined to a chromophore segment, as highlighted in red in Scheme 2.

Density Functional Theory Calculations. Density functional theory (DFT) calculations were applied to provide insight concerning the energies of various conformers for the ground and triplet excited states of the Pt−***n*** oligomers. In addition, time-dependent DFT (TD-DFT) calculations were used to provide insight concerning the effect of conformation on the S_0−S_1 transition. A large set of calculations were carried out on Pt−**2**, Pt−**3**, and Pt−**4** to explore the relative energies of ground-state conformers; the results obtained on the different oligomers were qualitatively similar; therefore, detailed results are presented herein only for Pt−**2**. In all of the calculations that are reported, the butyl chains on the PBu_3 ligands were truncated to methyls to facilitate the computations.

DFT was used to compute the energies of a variety of conformers for Pt−**2**. The structures were obtained either through geometry optimization without symmetry constraints or via optimization with specific symmetry constraints imposed. Energy minima for each stationary point were characterized either by the absence of imaginary frequencies or by the presence of a single imaginary low frequency corresponding to phenylene rotation. Table 1 lists the relative energies of six conformations of Pt−**2** that differ with respect to the orientation of the phenylene units. In general, the calculations demonstrate that the barrier to rotation around the C_{sp2}−C_{sp} or Pt−C_{sp} (subscripts indicate atomic hybridization) bonds is quite low (ca. 1 kcal·mol^{-1}). In this respect, the Pt−acetylides are very similar to oligo(phenylene ethynylene)s, where the barrier to rotation around the C_{sp2}−C_{sp} bonds is also ≤1 kcal·mol^{-1}.[59−61] The lowest-energy conformation is Pt−**2**−**ttt** in which the planes defined by the PtP_2C_2 units and the phenylenes are perpendicular. This finding is consistent with the conformations present in crystals of several Pt−acetylide oligomers.[62,63] In the crystals, the arylene units are rotated 60° or more relative to the planes defined by the PtP_2C_2 units. The DFT calculations on Pt−**2** indicate that the energy cost for rotating a terminal phenylene into the **p** conformation is ∼0.5 kcal·mol^{-1} whereas the energy cost for rotation of the central phenylene into the **p** conformation is ∼0.8 kcal·mol^{-1}. These effects are nearly additive, suggesting that for Pt−**2** there is a family of conformers that lie ≤2 kcal·mol^{-1}above the lowest-energy conformer that interconvert via rotation around the C_{sp2}−C_{sp} and Pt−C_{sp} bonds.

TABLE 1. Relative Energies of Conformers of Pt−2

conformer[a]	symmetry	electronic state	relative energy/ kcal·mol^{-1} [b]
ttt	C_{2h}	S_0	0
ptt	C_s	S_0	0.55
tpt	D_{2h}	S_0	0.77
ppt	C_s	S_0	1.10
ptp	D_{2h}	S_0	1.15
ppp	C_{2h}	S_0	1.45
tpt	D_{2h}	T_1	0
ttt	C_{2h}	T_1	3.1

[a] See the text for a definition of conformer nomenclature. [b] Energy-optimized structures using DFT with an SDD basis set.

The small rotational barrier is mostly due to steric factors, but electronic interactions also play a role. In particular, calculations carried out with PBu_3 rather than PMe_3 ligands showed a slight increase in the energy of **p** relative to **t** conformers. An inspection of the plots of the HOMOs for Pt−**2**−**ttt** and Pt−**2**−**tpt** (Supporting Information, Figure S-2) supports the premise that orbital interactions may also play a role in determining the lowest-energy conformation. In particular, for the **ttt** conformer there is a large extent of electronic delocalization across the entire oligomer, and coupling between the phenylene ethynylene units is mediated by the overlap of the p orbitals on the C_{sp} carbons with the in-plane Pt $5d_{xy}$ orbital. By contrast, in the **tpt** conformation the HOMO is more confined to the central phenylene unit, and there is overlap of the p orbitals on the C_{sp} carbons with the out-of-plane Pt $5d_{xz}$ and $6p_z$ orbitals.

Regardless of the origin of the effect, the preference for the twisted conformation extends to the other members of the Pt−***n*** series. Figure 5 illustrates the lowest-energy conformations computed by DFT for Pt−**2**, Pt−**3**, and Pt−**4**. In each case the "all-**t**" conformation is energetically preferred over conformers in which terminal or internal phenylenes are rotated into the **p** conformation.

DFT was also used to obtain the optimized geometry for the lowest triplet (excited) state in Pt−**2**, Pt−**3**, and Pt−**4**. Similar results were obtained for Pt−**2** and the longer oligomers, as outlined below. For each oligomer, the calculations strongly support the premise that the triplet is spatially confined. Figure 6 shows two conformations of the lowest triplet state of Pt−**2** along with calculated bond lengths. (The ground-state Pt−**2**−**ttt** structure is included in the figure for comparison.)

Interestingly, in the triplet state the **tpt** conformer is the energy minimum, whereas the **ttt** conformation lies ca. 3.1 kcal·mol^{-1} higher in energy (Table 1). Note that the relative energetic ordering of the conformations in the triplet state is inverted compared to that in the ground state. Moreover, the energy difference between the **p** and **t** conformers is substantially increased in the triplet state. Comparison of the bond lengths for the triplet Pt−**2**−**tpt** and ground-state Pt−**2**−**ttt** structures reveals that in the former there is a clear quinoidal geometric distortion that is concentrated in the central 1,4-diethynylphenylene unit.

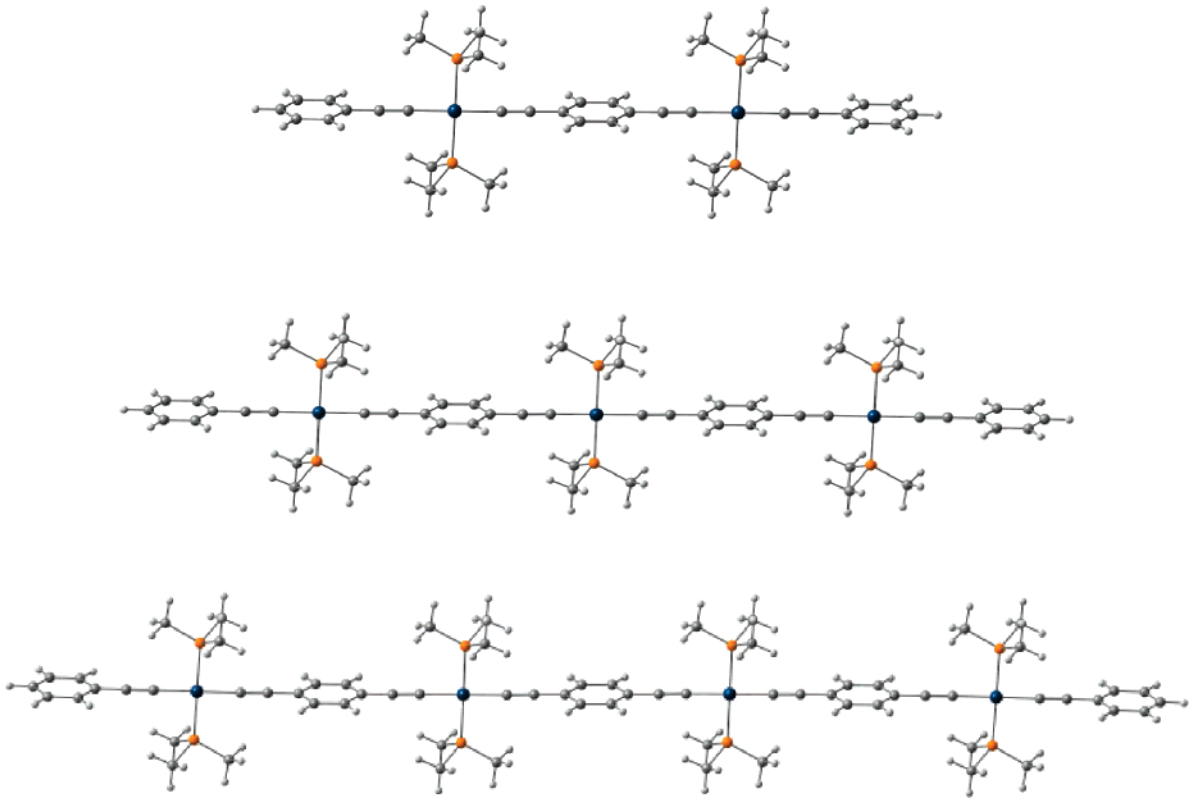

Figure 5. Geometry-optimized structures of Pt−**2** through Pt−**4** computed by DFT. Lowest-energy conformers are shown for each structure.

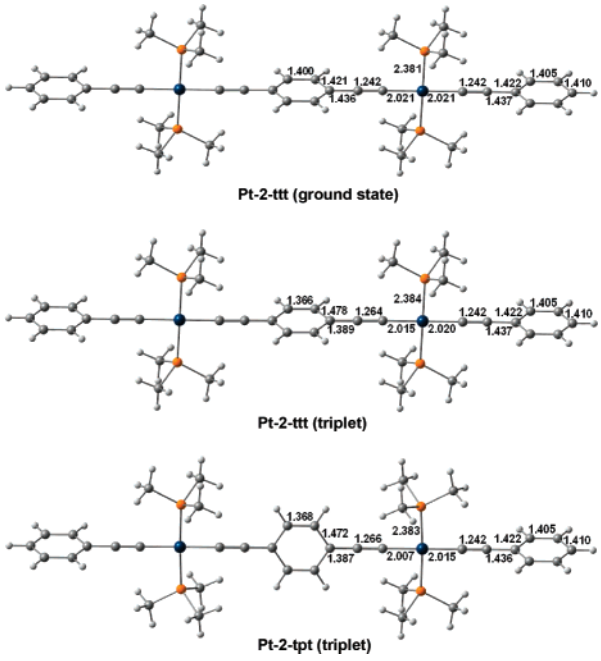

Figure 6. Geometry-optimized structures of Pt−**2**. (Bottom) Pt−**2**−**tpt**, lowest-energy conformation of triplet excited state (T_1). (Middle) Pt−**2**−**ttt**, triplet state (T_1), conformer lies 3 kcal·mol^{-1} above the **tpt** conformer. (Top) Pt−**2**−**ttt**, lowest-energy conformation of the ground state (S_0). Numbers show bond lengths in each structure.

Geometry optimization for the lowest triplet state in Pt−**4** results in a similar effect: the lowest-energy conformation is **ttptt**, where the central phenylene ring is rotated planar. This conformation is ca. 3 kcal·mol^{-1} lower in energy compared to that of the **ttttt** conformer. More insight into the structure of the triplet in Pt−**4** comes by comparing the bond lengths for the lowest-energy triplet- and ground-state conformations (Figure 7). This analysis shows that the geometry of the triplet differs from that of the ground state only in the core −[PtL_2−C≡C−Ph−C≡C−PtL_2]− unit. In particular, as shown by the structure and graph in the triplet state there is a quinoidal geometric distortion that is localized within the central 1,4-diethynylphenylene unit. It is important to note that the results of the calculation are entirely consistent with the spectroscopic studies of the triplet state, which led us to conclude that the triplet state in the Pt−acetylides is confined to a chromophore consisting of a single −[PtL_2−C≡C−Ph−C≡C−PtL_2]− unit.

Time Dependent DFT Calculations: Effects of Conformation on Transition Energies. TD-DFT calculations were carried out on several conformers of Pt−**2**, Pt−**3**, and Pt−**4** in order to provide insight into the relationship between the conformation of the conjugated chain and the energies of the S_0−S_1 and S_0−T_1 transitions. At the outset, it was hoped that the TD-DFT results would provide the basis with which to explain the experimental temperature-dependent absorption and phosphorescence data. Table 2 summarizes the results of the TD-DFT calculations. Before discussing these results in detail, it is important to point out that in general the TD-DFT results are in agreement with the experimental spectral data. For each of the oligomers, the calculations provide transition energies that are within 0.5 eV of the observed spectral bands.

The TD-DFT calculations show that in the all-**t** conformations of Pt−**2**, Pt−**3**, and Pt−**4** the S_0−S_1 transition is dominated by the HOMO−LUMO transition. The calculated transitions shift to lower energy with increasing oligomer length, and the calculated shifts are in good agreement with the experimentally observed red shift in the absorption bands. The results support the notion that in the Pt−actylide oligomers there is a substantial degree of delocalization in the singlet excited state.

To probe the effect of conformation on the S_0−S_1 transition energies, TD-DFT calculations were carried out on oligomers

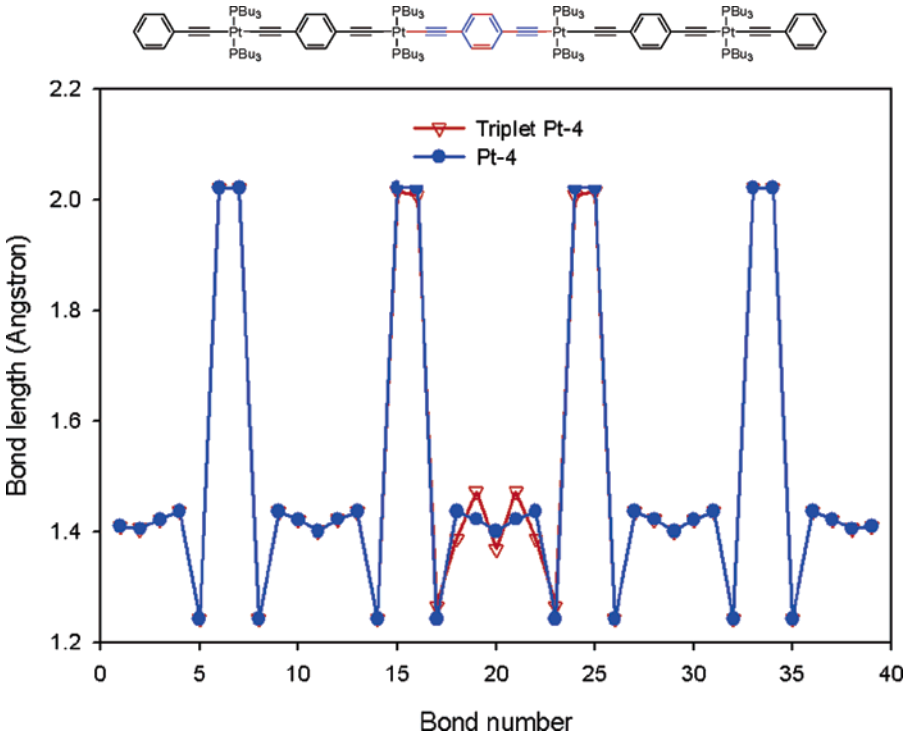

Figure 7. Plot showing bond lengths for Pt−**4** structures. X-axis labels indicate bond numbers starting from the para position of one of the terminal phenylene rings. (●) Pt−**4**, lowest-energy conformer of the ground state (S_0). (▽) Pt−**4**, lowest-energy conformer of the triplet state (T_1). Structure shown at top shows bonds that differ in length by more than 0.01 Å in the singlet and triplet states. Red bonds are shorter and blue bonds are longer in the triplet state.

TABLE 2. Results of TD-DFT Calculations on Pt−*n* Oligomers

	Singlet absorption					Triplet absorption on ground-state geometry		Triplet absorption on triplet-state geometry	
oligomer	orbital transitions	% contr.	calc. S_0-S_1, nm	calc. f in a.u.	exp. S_0-S_1, nm	calc. S_0-T_1, nm	calc. f in a.u.	calc. T_1-S_0, nm	exp. T_1-S_0, nm
Pt−**2**−**ttt**	H → L	100	319	2.1042	355	474	0	658	516
Pt−**2**−**tpt**	H → L	98	370	1.8025		511	0	695	
	H−3 → L + 2	2	370	1.8025		511	0	695	
Pt−**3**−**tttt**	H → L	96	331	3.2337	363	477	0	553[a]	517
	H−1 → L + 1	4	331	3.2337	363	477	0	553[a]	517
Pt−**3**−**tptt**	H → L	98	372	2.3981		511	0	695	
	H−5 → L + 4	2	372	2.3981		511	0	695	
Pt−**4**−**ttttt**	H → L	90	336	4.5028	367	478	0	658	518
	H−1 → L + 1	10	336	4.5028	367	478	0	658	518
Pt−**4**−**ttptt**	H → L	98	373	3.0397		511	0	695	
	H−13 → L + 7	2	373	3.0397		511	0	695	

[a] The C_{2h} symmetry of this structure forces the triplet to delocalize on both of the inner 1,4-phenylenediyl segments of Pt−3−tttt. Therefore, the calculated triplet emission wavelength is considerably different for this structure compared to those of other Pt−***n*** oligomers in this column.

with one of the phenyl groups in the **p** conformation. In particular, for Pt−**2**, Pt−**3**, and Pt−**4** the S_0-S_1 transition energy was computed for the **tpt**, **tptt**, and **ttptt** conformers, respectively. Interestingly, the results show that in each case the rotation of a single phenylene unit into the **p** conformer results in a substantial lowering of the S_0-S_1 transition energy. For Pt−**2**, Pt−**3**, and Pt−**4**, the S_0-S_1 transition is shifted to lower energy by 0.53, 0.41, and 0.37 eV, respectively. An important point is that the TD-DFT computed difference in the S_0-S_1 transition for the all-**t** conformers relative to those that contain a phenylene unit in the **p** conformation is very similar to the shift in the experimental absorption spectra of the oligomers as the temperature is decreased from ambient to 80 K (Figure 1).

Two different TD-DFT methods were used to compute the S_0-T_1 energy gap. Specifically, calculations were carried out using the DFT-optimized ground-state geometry and the DFT-optimized triplet-state geometry. In each case, calculations were made for the all-**t** conformers and for structures in which one phenylene unit is in the **p** conformation. The S_0-T_1 transition energies computed using the ground-state geometry are in remarkably good agreement with the experimentally observed phosphorescence energies, whereas those computed using the triplet geometry underestimate the experimental energy by ca. 0.5 eV. Regardless of which geometry is used, the TD-DFT calculations indicate that the S_0-T_1 transition energy is affected very little by oligomer length. This result is in agreement with experiment and supports the notion that the triplet exciton is strongly confined in the Pt−acetylide oligomers.

The TD-DFT calculations suggest that the conformation of the phenylene units has a similar effect on the S_0-T_1 transitions as described above for the S_0-S_1 transitions. In particular, for Pt−**2** computed S_0-T_1 transition shifts are from 474 nm for

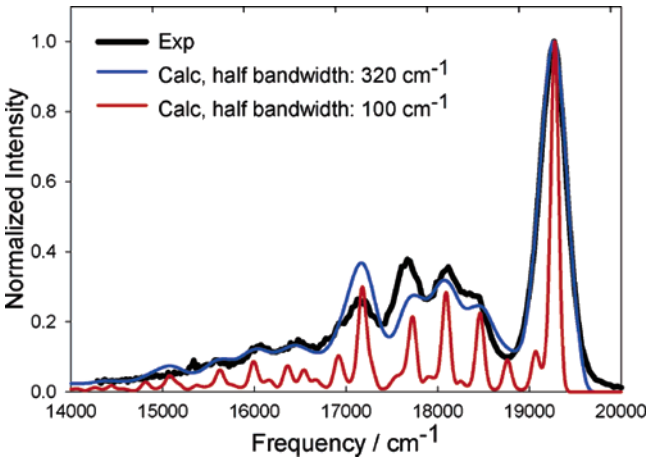

Figure 8. Comparison of experimental (black) and calculated phosphorescence spectra of Pt−**2**. Spectra are computed using the seven vibronic modes shown in Figure S-3 (Supporting Information) according to the procedure described in ref 49. Huang−Rhys factors are multiplied by 2 in the simulated spectra to facilitate comparison of the computed and experimental spectra.

the **ttt** conformer to 511 nm for the **tpt** conformer. (For calculations on ground-state geometry, the shift corresponds to 0.18 eV or 4.1 kcal·mol^{-1}.) Similar shifts of the S_0-T_1 transition energy are seen for the other oligomers as one phenylene unit is rotated into the **p** conformation. It is interesting that the calculated shift in the S_0-T_1 transition energy corresponds very closely to the difference in energy between the two emission bands seen for Pt−**2** and Pt−**3** in the frozen 2-MTHF solvent glass ($\Delta E \approx 4.2$ kcal·mol^{-1}).

Discussion

Structure of the Triplet Exciton in Platinum−Acetylide Oligomers. The experimental results presented above provide compelling evidence that the triplet exciton in the Pt−***n*** oligomers is localized to a short segment length. First, as pointed out in our previous communication,[42] the phosphorescence energy shifts very little across the entire series. Second, the quantitative transient absorption spectroscopy data presented in this study further supports the notion of triplet localization. In particular, the absolute absorption spectrum of the triplet state in Pt−**2** features little absorptivity in the 350−400 nm region. This shows that in the short oligomer the ground-state absorption (S_0-S_1) is completely depleted in the excited state, which is consistent with the idea that in the Pt−**2** the triplet chromophore encompasses the entire oligomer. However, as the oligomer length increases, the triplet-state absorption spectrum shows increasing absorptivity in the 350−400 nm region. This demonstrates that in the longer oligomers the ground-state absorption is incompletely bleached, which is consistent with the notion that the triplet exciton is confined to a small segment of the oligomer chain. In essence, the residual absorption that appears in the 350−400 nm region for the longer oligomers is the S_0-S_1 transition in the unexcited segment of the oligomer. As noted above, on the basis of the spectroscopic results we postulate that the triplet exciton encompasses the chromophore illustrated in Scheme 2.

The DFT calculations are in complete accord with our model of triplet exciton localization in the Pt−***n*** oligomers. First, clear evidence of triplet localization comes from the similarity between the calculated vibronic progression in the phosphorescence spectrum and the experimental emission spectrum of Pt−**2** (Figure 8). The simulated spectrum was obtained using the triplet- Pt−**2**−**tpt** and ground-state Pt−**2**−**tpt** geometries. Among the large number of normal modes for ground-state Pt−**2**−**tpt**, only those modes with a_g symmetry serve as coupling modes for the $T_1 \rightarrow S_0$ transition. In the calculated spectrum, we used the seven vibrational modes that display relatively large Huang−Rhys constants ($S \geq 0.08$).[49] These modes are located at 93, 216, 533, 835, 1213, 1648, and 2165 cm^{-1}, and they are illustrated in Figure S-3 in the Supporting Information. As shown in Figure 8, the position of the primary vibrational subbands agrees very well with the experimental spectrum; however, the calculation underestimates the intensity of the subbands. This indicates that the calculated Huang−Rhys constants are underestimated possibly as a result of the neglect of the effect of the phenylene torsional modes on the Huang−Rhys factors.[64]

The important point with respect to triplet-state structure is that, as shown in Figure S-3, all of the vibrational modes above 533 cm^{-1} that are coupled to the $T_1 \rightarrow S_0$ transition are localized on the central 1,4-diethynylphenylene unit. This fact emphasizes that the triplet chromophore can be represented by Scheme 2.

The calculations also provide insight into the difference in geometry between the ground and triplet excited states. In particular, the calculations indicate that in the ground state there is a relatively low barrier for rotation of the phenylene units around the oligomer axis. The calculations also suggest (but do not prove) that in the ground state the all-**t** conformation is most stable. By contrast, the DFT calculations suggest that in the triplet state there is a significant quinoidal geometric distortion in a single $-[PtL_2-C\equiv C-Ph-C\equiv C-PtL_2]-$ unit that comprises the triplet chromophore (Figures 6 and 7). In addition, the phenylene unit in the triplet chromophore is in the **p** conformation, and there is a substantially larger barrier for rotation of this phenylene unit in the triplet state: the **t** conformation of the triplet is 3 kcal·mol^{-1} above the **p** conformation.

This model of a localized triplet exciton brings with it the possibility that in a longer oligomer (or in a polymer) the triplet exciton may diffuse along a chain via hopping between adjacent triplet chromophore segments. Triplet exciton hopping may be accompanied by a small activation energy arising from a reorganizational energy that is caused by the geometric difference between the triplet- and ground-state Pt−acetylide chromophores.

The phenomenon of triplet exciton hopping was explored in a recent investigation of a series of Pt−acetylide copolymers.[57] The results of this study suggest that at ambient temperature triplet exciton hopping among triplet chromophores along a chain occurs very rapidly ($\tau < 1$ ns); however, at cryogenic temperatures in a rigid solvent glass, triplet exciton hopping is slowed such that it is competitive with the exciton lifetime ($\tau \approx \mu$s).[57] This slowing of triplet exciton hopping at low temperature is consistent with the notion that the process has a small to moderate activation energy (i.e., in the range of 3−5 kcal·mol^{-1}). Note that this is in accord with the DFT calculations that suggest that in the triplet state the energy difference between the **t** and **p** conformers is ca. 3 kcal·mol^{-1}. The concept of hopping of a localized triplet exciton along an oligomer chain will be used below as we explain some of the spectroscopic results.

Model to Explain Temperature Dependence of Absorption and Phosphorescence. At this point, we develop a model to explain the most significant experimental observations of this work: (1) with decreasing temperature, the absorption spectra of the Pt−***n*** oligomers red shift and narrow in bandwidth and

(2) at low temperatures in a solvent glass, the phosphorescence of the short oligomers (Pt−**2** and Pt−**3**) is split into two components, whereas for the longer oligomers the splitting is less evident. First, in a general sense it is clear that the changes in the absorption and phosphorescence spectra arise as a result of the effect of temperature on the conformation of the oligomers. In the ground state, the barrier for interconversion of the **t** and **p** conformers is very low; consequently, at ambient temperature the oligomers exist in a large number of conformations that are able to interconvert rapidly. However, as the temperature decreases the conformational equilibrium shifts so that the more stable conformation predominates and conjugation along the oligomer backbone increases. Finally, as the temperature falls below the solvent glass point (ca. 120−130 K in the present work), the oligomers are frozen in a state where some conformational disorder may remain (i.e., **t**−**p** interconversion is prevented).

A shift in conformer equilibrium with decreasing temperature explains the red shift that occurs in the absorption spectra with decreasing temperature. On the basis of the ground-state DFT calculations, one would predict that as the temperature decreases the all-**t** conformation will begin to predominate (Table 1). However, this prediction leads to a contradiction: The TD-DFT calculations indicate that **t** conformers absorb at higher energy (blue shift) relative to the **p** conformers. In apparent conflict with this is the fact that the experimental absorption spectra red shift with decreasing temperature, *opposite* to the direction of the shift that is expected if the all-**t** conformers predominate at low temperature. Given the very clear result from the TD-DFT calculations, which show that **p** conformers absorb at considerably lower energy than do **t** conformers, we believe that the experimental absorption results must be interpreted as showing that **p** conformers predominate at low temperature.

The apparent discrepancy between the theoretical and experimental results led us to carry out a more thorough DFT investigation to determine whether the lowest-energy conformer is **t** or **p**. Possible sources of error considered include (1) an inadequate theoretical approach, (2) neglect of vibronic- and thermal-energy corrections to the total energy, and (3) neglect of solvent stabilization. First, several other theoretical methods were employed to examine the effect of the method and basis set used for determining the energy difference between **p** and **t** conformers.[65] All of these calculations indicate that the **t** conformer is the lowest-energy structure with **t**−**p** energy differences similar to those obtained from the B3LYP/SDD calculations. Next, we incorporated zero-point energy (ZPE) and thermal energy corrections to the enthalpy of each conformer (Pt−**2**−**ttt** and Pt−**2**−**tpt**) from frequency calculations. These results show that by including the thermal energy and ZPE correction to the enthalpy $\Delta H_{\mathbf{t}\rightarrow\mathbf{p}}$ decreases to 0.04 kcal·mol^{-1} indicating that there is almost no preference of one conformer over another at room temperature. The calculated entropy difference is $\Delta S_{\mathbf{t}\rightarrow\mathbf{p}} = -9$ cal·mol^{-1}·K^{-1}, which slightly favors the shift of equilibrium to the Pt−**2**−**ttt** conformer at room temperature; however, with decreasing temperature the entropy term becomes negligible, and thus the equilibrium may begin to favor the Pt−**2**−**tpt** conformer.

Finally, we consider the solvent effect on the equilibrium of **t** → **p** interconversion. Although there is little difference between the energy of the two conformers in the gas phase, it is possible that in solution the **p** conformer is stabilized more than the **t** conformer. Polarized continuum model (PCM) calculations on the gas-phase optimized structures of Pt−**2**−**ttt** and Pt−**2**−**tpt** indicate that the latter is more stable in solution by ca. 3 kcal·mol^{-1}. Although the PCM results are not definitive (because the structures were not optimized in the presence of the solvent), they clearly show that solvent effects may be a possible explanation for the apparent stabilization of the **p** conformer in 2-MTHF.

We now explain the observed temperature-dependence effects on the phosphorescence spectra of the oligomers. First, for all of the oligomers at temperatures above the glass point of the solvent the phosphorescence has a single 0−0 band with a clear vibronic progression. Here, we use Pt−**2** as an example to explain this observation, but the effects are the same in the longer oligomers. Vertical excitation of the all-**t** conformation, Pt−**2**−**ttt**, affords the Franck−Condon excited state, *Pt−**2**−**ttt**. This state rapidly undergoes conformational isomerization to produce the relaxed triplet state, *Pt−**2**−**tpt**. On a longer time scale, the relaxed triplet decays via radiative and nonradiative decay. In fluid solution, conformational relaxation is rapid; consequently, phosphorescence is observed only from the relaxed triplet state (i.e., the **p** conformation), which explains why only a single phosphorescence origin is observed in the spectra of all of the oligomers at ambient temperature.

As noted above, at low temperature the oligomers exist preferentially in the **p** conformational state. However, there is still likely to be some conformational heterogeneity present, that is, some oligomer repeat will exist in the **t** conformation. When the temperature falls below the solvent glass point, the conformational distribution is frozen on the time scale of the triplet lifetime. For Pt−**2** in the frozen glass, there will essentially be two distinct populations of molecules with conformations that will phosphoresce at different energies—those with the central phenylene ring in the **t** and those with the **p** conformation. These two conformers are the origin of the distinct emission and excitation spectra that are shown in Figure 3. In particular, Pt−**2** oligomers with the central phenylene in the **t** conformation exhibit the blue-shifted phosphorescence and absorption (excitation) spectra, whereas those with phenylene in the **p** conformation exhibit the red-shifted spectra. For the longer oligomers in the frozen glass, there will still be some oligomer repeat units that are frozen in the **t** conformation. However, the likelihood that an oligomer will exist in the all-**t** conformation will decrease with increasing oligomer length. Thus, when a longer oligomer is photoexcited, if the triplet exciton happens to be initially produced on a repeat unit in the **t** conformation, then it can simply hop via intramolecular energy transfer to a nearby triplet chromophore that is in the **p** conformation. The ability of the triplet exciton to migrate in the longer oligomers explains why at low temperature phosphorescence spectra show little evidence for emission from the higher-energy state that is so prominent in the low-temperature spectra of Pt−**2** and Pt−**3**.

Summary and Conclusions

We have carried out a comprehensive experimental and theoretical investigation that examined the properties of the ground and excited states of the series of Pt−***n*** oligomers. This study was focused on exploring the electronic and geometric structures of the ground and triplet excited states and how these factors are affected by oligomer length.

The π, π^* absorption band of the oligomers occurs in the near-UV, and the band red shifts substantially with decreasing temperature over the 298−80 K range. All of the oligomers exhibit phosphorescence with a 0−0 band maximum near 520 nm. Temperature-dependence studies show that the phosphorescence energy and band shape do not change substantially with temperature until the solvent glass point is reached. Below

the solvent glass temperature, in the short oligomers (Pt−**2** and Pt−**3**) the 0−0 band splits, and a second band is observed that is blue-shifted slightly compared to the main 0−0 band (i.e., at higher energy). The splitting of the phosphorescence band in the solvent glass is not seen in the longer oligomers.

Transient absorption spectroscopy was applied to obtain the absolute triplet−triplet absorption spectra of the oligomers in solution at ambient temperature. For all of the oligomers, the triplet state exhibits a strong triplet−triplet absorption band with $\lambda_{max} \approx 650$ nm and $\epsilon_{max} \approx (60-80) \times 10^3$ $M^{-1}\cdot cm^{-1}$. For the longer oligomers, there is an additional band that appears in the triplet absorption spectrum in the same region where the ground-state absorption arises. These observations are consistent with the triplet state being localized to a chromophore consisting of $-[PtL_2-C\equiv C-Ph-C\equiv C-PtL_2]-$.

Quantum calculations were carried out on the Pt−***n*** oligomers using DFT and TD-DFT to provide insight concerning the origin of the experimental observations. The DFT calculations indicate that in the ground state there is a small energy difference (<1 kcal·mol^{-1}) between the **p** and **t** conformers. This finding indicates that in fluid solution the oligomers exist as a heterogeneous population consisting of different conformers that differ with respect to rotation around the $Pt-C_{sp}$ and $C_{sp}-C_{Ar}$ bonds. By contrast, in the triplet excited state the **p** conformer is 3 kcal·mol^{-1} lower in energy compared to the **t** conformer, and the analysis of the triplet geometry and vibrational mode structure strongly suggests that the triplet is localized on a single $-[PtL_2-C\equiv C-Ph-C\equiv C-PtL_2]-$ unit. TD-DFT calculations clearly indicate that the S_0-S_1 absorption occurs at higher energy in **t** conformers relative to **p** conformers. This theoretical result leads us to conclude that the experimentally observed red shift in the absorption bands with decreasing temperature means that the **p** conformers are predominant in the conformer population at low temperature (T < 150 K).

The splitting of the phosphorescence 0−0 band in the short oligomers at low temperature in the solvent glass is ascribed to emission from **t** and **p** conformers that cannot interconvert in the frozen matrix. This effect is not seen in the longer oligomers (Pt−**4** and longer); this effect is ascribed to intrachain energy transfer that allows an exciton to relax by migrating to a repeat unit in the **p** conformation.

The most significant result of this work is that it provides unambiguous evidence for triplet localization in Pt−acetylide oligomers. Although the concept of triplet localization in organic and organometallic conjugated oligomers and polymers has been explored in a number of investigations,[29,37,66−68] the work presented herein provides a very clear experimental and theoretical description of the effect. Although this work highlights the importance of localization in determining the spectroscopic properties of the triplet state in Pt−acetylide oligomers, a question that remains concerns the dynamics of intrachain triplet exciton transport. This effect is the focus of ongoing investigations in our laboratories and will be the subject of future communications.

Acknowledgment. We gratefully acknowledge the National Science Foundation (grant no. CHE-0515066) for supporting this work.

Supporting Information Available: Transient absorption spectra and decays for energy-transfer studies of Pt−**3** and pyrene, HOMO and LUMO orbital plots for Pt−**2**−**ttt** and Pt−**2**−**tpt**, and vibrational modes coupled to T_1-S_0 decay. This material is available free of charge via the Internet at http://pubs.acs.org.

References and Notes

(1) Burroughes, J. H.; Bradley, D. D. C.; Brown, A. R.; Marks, R. W.; Mackay, K.; Friend, R. H.; Burn, P. L.; Holmes, A. B. *Nature* **1990**, *347*, 539−541.

(2) Kraft, A.; Grimsdale, A. C.; Holmes, A. B. *Angew. Chem., Int. Ed.* **1998**, *37*, 402−428.

(3) Groenendaal, B. L.; Jonas, F.; Freitag, D.; Pielartzik, H.; Reynolds, J. R. *Adv. Mater.* **2000**, *12*, 481−494.

(4) Yu, G.; Gao, J.; Hummelen, J. C.; Wudl, F.; Heeger, A. J. *Science* **1995**, *270*, 1789−1791.

(5) Skotheim, T. A.; Elsenbaumer, R. L.; Reynolds, J. R., Eds. *Handbook of Conducting Polymers*, 2nd ed.; Marcel Dekker: New York, 1998.

(6) McGehee, M. D.; Miller, E. K.; Moses, D.; Heeger, A. J. In *Advances in Synthetic Metals: Twenty Years of Progress in Science and Technology*; Bernier, P., Lefrant, S., Bidan, G., Eds.; Elsevier: Amsterdam, 1999; pp 98−205.

(7) Martin, R. E.; Diederich, F. *Angew. Chem., Int. Ed.* **1999**, *38*, 1350−1377.

(8) Tour, J. M. *Chem. Rev.* **1996**, *96*, 537−554.

(9) Baldo, M. A.; Thompson, M. E.; Forrest, S. R. *Nature* **2000**, *403*, 750−753.

(10) Lamansky, S.; Djurovich, P.; Murphy, D.; Abdel-Razzaq, F.; Lee, H. E.; Adachi, C.; Burrows, P. E.; Forrest, S. R.; Thompson, M. E. *J. Am. Chem. Soc.* **2001**, *123*, 4304−4312.

(11) Evans, R. C.; Douglas, P.; Winscom, C. J. *Coord. Chem. Rev.* **2006**, *250*, 2093−2126.

(12) Shao, Y.; Yang, Y. *Adv. Mater. (Weinheim, Ger.)* **2005**, *17*, 2841−2844.

(13) Guo, F.; Kim, Y.-G.; Reynolds, J. J.; Schanze, K. S. *Chem. Commun.* **2006**, 1887−1889.

(14) McKay, T. J.; Bolger, J. A.; Staromlynska, J.; Davy, J. R. *J. Chem. Phys.* **1998**, *108*, 5537−5541.

(15) Staromlynska, J.; McKay, T. J.; Bolger, J. A.; Davy, J. R. *J. Opt. Soc. Am. B* **1998**, *15*, 1731−1736.

(16) Powell, C. E.; Humphrey, M. G. *Coord. Chem. Rev.* **2004**, *248*, 725−756.

(17) Kim, K.-Y.; Farley, R.; Schanze, K. S. *J. Phys. Chem. B*, published online Aug 12, http://dx.doi.org/10.1021/jp063916m.

(18) Kavandi, J.; Callis, J.; Gouterman, M.; Khalil, G.; Wright, D.; Green, E.; Burns, D.; McLachlan, B. *Rev. Sci. Instrum.* **1990**, *61*, 3340−3347.

(19) Furuta, P. T.; Deng, L.; Garon, S.; Thompson, M. E.; Frechet, J. M. J. *J. Am. Chem. Soc.* **2004**, *126*, 15 388−15 389.

(20) Wong, W.-Y.; Ho, C.-L. *Coord. Chem. Rev.* **2006**, *250*, 2627−2690.

(21) Sonogashira, K.; Takahashi, H.; Hagihara, N. *Macromolecules* **1977**, *10*, 879−880.

(22) Khan, M. S.; Kakkar, A. K.; Long, N. J.; Lewis, J.; Raithby, P.; Nguyen, P.; Marder, T. B.; Wittmann, F.; Friend, R. H. *J. Mater. Chem.* **1994**, *4*, 1227−1232.

(23) Chawdhury, N.; Kohler, A.; Friend, R. H.; Younus, M.; Long, N. J.; Raithby, P. R.; Lewis, J. *Macromolecules* **1998**, *31*, 722−727.

(24) Wilson, J. S.; Dhoot, A. S.; Seeley, A. J. A. B.; Khan, M. S.; Kohler, A.; Friend, R. H. *Nature* **2001**, *413*, 828−831.

(25) Dray, A. E.; Wittmann, F.; Friend, R. H.; Donald, A. M.; Khan, M. S.; Lewis, J.; Johnson, B. F. G. *Synth. Met.* **1991**, *41*, 871−874.

(26) Johnson, B. F. G.; Kakkar, A. K.; Khan, M. S.; Lewis, J.; Dray, A. E.; Friend, R. H.; Wittmann, F. *J. Mater. Chem.* **1991**, *1*, 485−486.

(27) Lewis, J.; Khan, M. S.; Kakkar, A. K.; Johnson, B. F. G.; Marder, T. B.; Fyfe, H. B.; Wittmann, F.; Friend, R. H.; Dray, A. E. *J. Organomet. Chem.* **1992**, *425*, 165−176.

(28) Wittmann, H. F.; Friend, R. H.; Khan, M. S.; Lewis, J. *J. Chem. Phys.* **1994**, *101*, 2693−2698.

(29) Beljonne, D.; Wittmann, H. F.; Kohler, A.; Graham, S.; Younus, M.; Lewis, J.; Raithby, P. R.; Khan, M. S.; Friend, R. H.; Bredas, J. L. *J. Chem. Phys.* **1996**, *105*, 3868−3877.

(30) James, S. L.; Younus, M.; Raithby, P. R.; Lewis, J. *J. Organomet. Chem.* **1997**, *543*, 233−235.

(31) Lewis, J.; Long, N. J.; Raithby, P. R.; Shields, G. P.; Wong, W. Y.; Younus, M. *J. Chem. Soc., Dalton Trans.* **1997**, 4283−4288.

(32) Chawdhury, N.; Younus, M.; Raithby, P. R.; Lewis, J.; Friend, R. H. *Opt. Mater.* **1998**, *9*, 498−501.

(33) Younus, M.; Kohler, A.; Cron, S.; Chawdhury, N.; Al-Mandhary, M. R. A.; Khan, M. S.; Lewis, J.; Long, N. J.; Friend, R. H.; Raithby, P. R. *Angew. Chem., Int. Ed.* **1998**, *37*, 3036−3039.

(34) Chawdhury, N.; Kohler, A.; Friend, R. H.; Wong, W. Y.; Lewis, J.; Younus, M.; Raithby, P. R.; Corcoran, T. C.; Al-Mandhary, M. R. A.; Khan, M. S. *J. Chem. Phys.* **1999**, *110*, 4963−4970.

(35) Wilson, J. S.; Kohler, A.; Friend, R. H.; Al-Suti, M. K.; Al-Mandhary, M. R. A.; Khan, M. S.; Raithby, P. R. *J. Chem. Phys.* **2000**, *113*, 7627−7634.

(36) Wilson, J. S.; Chawdhury, N.; Al-Mandhary, M. R. A.; Younus, M.; Khan, M. S.; Raithby, P. R.; Kohler, A.; Friend, R. H. *J. Am. Chem. Soc.* **2001**, *123*, 9412−9417.

(37) Kohler, A.; Wilson, J. S.; Friend, R. H.; Al-Suti, M. K.; Khan, M. S.; Gerhard, A.; Bassler, H. *J. Chem. Phys.* **2002**, *116*, 9457−9463.

(38) Khan, M. S.; Al-Mandhary, M. R. A.; Al-Suti, M. K.; Hisahm, A. K.; Raithby, P. R.; Ahrens, B.; Mahon, M. F.; Male, L.; Marseglia, E. A.; Tedesco, E.; Friend, R. H.; Kohler, A.; Feeder, N.; Teat, S. J. *J. Chem. Soc., Dalton Trans.* **2002**, 1358−1368.

(39) Khan, M. S.; Al-Mandhary, M. R. A.; Al-Suti, M. K.; Feeder, N.; Nahar, S.; Kohler, A.; Friend, R. H.; Wilson, P. J.; Raithby, P. R. *J. Chem. Soc., Dalton Trans.* **2002**, 2441−2448.

(40) Khan, M. S.; Al-Mandhary, M. R. A.; Al-Suti, M. K.; Corcoran, T. C.; Al-Mahrooqi, Y.; Attfield, J. P.; Feeder, N.; David, W. I. F.; Shankland, K.; Friend, R. H.; Kohler, A.; Marseglia, E. A.; Tedesco, E.; Tang, C. C.; Raithby, P. R.; Collings, J. C.; Roscoe, K. P.; Batsanov, A. S.; Stimson, L. M.; Marder, T. B. *New J. Chem.* **2003**, *27*, 140−149.

(41) Zhang, N.; Hayer, A.; Al-Suti, M. K.; Al-Belushi, R. A.; Khan, M. S.; Kohler, A. *J. Chem. Phys.* **2006**, *124*, 244701.

(42) Liu, Y.; Jiang, S. J.; Glusac, K.; Powell, D. H.; Anderson, D. F.; Schanze, K. S. *J. Am. Chem. Soc.* **2002**, *124*, 12 412−12 413.

(43) Wang, Y. S.; Schanze, K. S. *Chem. Phys.* **1993**, *176*, 305−319.

(44) Carmichael, I.; Hug, G. L. *J. Phys. Chem. Ref. Data* **1986**, *15*, 1−250.

(45) Frisch, M. J.; Trucks, G. W.; Schlegel, H. B.; Scuseria, G. E.; Robb, M. A.; Cheeseman, J. R.; Montgomery, J. A., Jr.; Vreven, T.; Kudin, K. N.; Burant, J. C.; Millam, J. M.; Iyengar, S. S.; Tomasi, J.; Barone, V.; Mennucci, B.; Cossi, M.; Scalmani, G.; Rega, N.; Petersson, G. A.; Nakatsuji, H.; Hada, M.; Ehara, M.; Toyota, K.; Fukuda, R.; Hasea, J.; Ishida, M.; Nakajima, T.; Honda, Y.; Kitao, O.; Nakai, H.; Klene, M.; Li, X.; Knox, J. E.; Hratchian, H. P.; Cross, J. B.; Bakken, V.; Adamo, C.; Jaramillo, J.; Gomperts, R.; Stratmann, R. E.; Yazyev, O.; Austin, A. J.; Cammi, R.; Pomelli, C.; Ochterski, J. W.; Ayala, P. Y.; Morokuma, K.; Voth, G. A.; Salvador, P.; Dannenberg, J. J.; Zakrzewski, V. G.; Dapprich, S.; Daniels, A. D.; Strain, M. C.; Farkas, O.; Malick, D. K.; Rabuck, A. D.; Raghavachari, K.; Foresman, J. B.; Ortiz, J. V.; Cui, Q.; Baboul, A. G.; Clifford, S.; Cioslowski, J.; Stefanov, B. B.; Liu, G.; Liashenko, A.; Piskorz, P.; Komaromi, I.; Martin, R. L.; Fox, D. J.; Keith, T.; Al-Laham, M. A.; Peng, C. Y.; Nanayakkara, A.; Challacombe, M.; Gill, P. M. W.; Johnson, B.; Chen, W.; Wong, M. W.; Gonzalez, C.; Pople, J. A. *Gaussian 03*, revision C.02; Gaussian, Inc.: Wallingford, CT, 2004.

(46) Becke, A. D. *Phys. Rev. A*: *At., Mol., Opt. Phys.* **1988**, *38*, 3098−3100.

(47) Lee, C.; Yang, W.; Parr, R. G. *Phys. Rev. B: Condens. Matter* **1988**, *37*, 785−789.

(48) Becke, A. D. *J. Chem. Phys.* **1993**, *98*, 5648−5652.

(49) Gierschner, J.; Mack, H. G.; Luer, L.; Oelkrug, D. *J. Chem. Phys.* **2002**, *116*, 8596−8609.

(50) In the conformers considered in the course of this investigation, all of the square-planar *trans*-$Pt(PBu_3)_2(C)_2$ units are oriented coplanar.

(51) Yang, C.; Orfino, F. P.; Holdcroft, S. *Macromolecules* **1996**, *29*, 6510−6517.

(52) Walters, K. A.; Ley, K. D.; Schanze, K. S. *Langmuir* **1999**, *15*, 5676−5680.

(53) Miteva, T.; Palmer, L.; Kloppenburg, L.; Neher, D.; Bunz, U. H. F. *Macromolecules* **2000**, *33*, 652−654.

(54) Principal component analysis was performed on a personal computer with a macro written in Matlab. A nonorthogonal target transformation was applied in order to obtain the real eigenvectors that correspond to the phosphorescence spectra of the principal components (See ref. 55 for the general approach used.)

(55) Saltiel, J.; Sears, D. F.; Sun, Y. P.; Choi, J. O. *J. Am. Chem. Soc.* **1992**, *114*, 3607−3612.

(56) Haskins-Glusac, K. Photophysics of Platinum−Acetylides. Ph.D. Dissertation, University of Florida, Gainesville, FL, 2003, http://www.chem.ufl.edu/~kschanze/dissertations.htm.

(57) Schanze, K. S.; Silverman, E. E.; Zhao, X. *J. Phys. Chem. B* **2005**, *109*, 18 451−18 459.

(58) Rogers, J. E.; Cooper, T. M.; Fleitz, P. A.; Glass, D. J.; McLean, D. G. *J. Phys. Chem. A* **2002**, *106*, 10 108−10 115.

(59) Young, J. K.; Moore, J. S. Acetylenes in Nanostructures. In *Modern Acetylene Chemistry*; Diederich, F., Stang, P. J., Eds.; VCH: Weinheim, Germany, 1995; Chapter 12.

(60) Magyar, R. J.; Tretiak, S.; Gao, Y.; Wang, H. L.; Shreve, A. P. *Chem. Phys. Lett.* **2005**, *401*, 149−156.

(61) James, P. V.; Sudeep, P. K.; Suresh, C. H.; Thomas, K. G. *J. Phys. Chem. A* **2006**, *110*, 4329−4337.

(62) Davy, J.; Gunter, M. E.; Tiekink, E. R. T. *Z. Kristallogr.* **1998**, *213*, 483−486.

(63) Haskins-Glusac, K.; Ghiviriga, I.; Abboud, K. A.; Schanze, K. S. *J. Phys. Chem. B* **2004**, *108*, 4969−4978.

(64) As stated earlier, in the ground-state phenylene rotation has a very low energy barrier. Therefore, the ground state Pt−**2**−**tpt** structure used in the simulations does not reflect the true equilibrium geometry of the ground state. We attempted to use the Pt−**2**−**ttt** conformation in the spectral simulations; however, in this case the calculated Huang−Rhys factors become unrealistically high as a result of the large geometry change of the central phenylene ring that accompanies the T_1(Pt−**2**−**tpt**) to S_0(Pt−**2**−**ttt**) transition. Nevertheless, this calculation demonstrates the importance of low-frequency modes in simulating the relative intensity of the vibronic subbands.

(65) The PW91/SDD, PW91/LanL2DZ, HF/SDD, B3LYP/SDD (for Pt) /6-31.g(d,p) (for other atoms), and B3LYP/LanL2DZ (for Pt) /6-31.g(d,p) (for other atoms) methods all suggest that the t conformer is the most stable with energy differences varying from 0.17 to 0.69 kcal·mol^{-1} with respect to the p conformer.

(66) McGlynn, S. P.; Smith, F. J.; Cilento, G. *Photochem. Photobiol.* **1964**, *3*, 269−294.

(67) Wasserberg, D.; Dudek, S. P.; Meskers, S. C. J.; Janssen, R. A. J. *Chem. Phys. Lett.* **2005**, *411*, 273−277.

(68) Batista, E. R.; Martin, R. L. *J. Phys. Chem. A* **2005**, *109*, 9856−9859.